Corrosion Inhibition of Carbon Steel in Hydrochloric Acid Solution Using a Sulfa Drug

A. Samide,[a,*] B. Tutunaru,[a] and C. Negrila[b]
[a]University of Craiova, Faculty of Chemistry,
Calea Bucuresti 107i, Craiova, Romania
[b]National Institute of Materials Physics,
077125 Magurele-Bucharest, Romania

Original scientific paper
Received: April 10, 2011
Accepted: September 12, 2011

The corrosion inhibition of carbon steel in 1.0 mol L^{-1} HCl in the presence of an antibacterial sulfa drug Sulfathiazole, IUPAC name 4-amino-N-(1,3-thiazol-2-yl) benzene sulfonamide (TBSA) was investigated using mass loss and electrochemical measurements such as: potentiodynamic polarization and electrochemical impedance spectroscopy (EIS). Surface chemistry was analyzed by X-ray photoelectron spectroscopy (XPS). For the study of the surface morphology scanning electron spectroscopy (SEM) was used. The results showed that TBSA acts as a corrosion inhibitor in 1.0 mol L^{-1} HCl solution by suppressing simultaneously the cathodic and anodic processes *via* adsorption on the carbon steel surface and that the inhibition efficiency increases with increasing concentration. XPS analysis revealed that the corrosion product consists of an oxyhydroxide/oxide mixture and that the iron oxyhydroxide proportion is higher than the iron oxide proportion.

Key words:
Carbon steel, corrosion inhibition, mass loss, EIS, SEM, XPS

Introduction

Steel is widely used in most industries because of its special properties. However, the metal corrodes when it comes in contact with different corrosive media[1–8] and different environments require versatile inhibition actions.[9]

Several inhibitors in use are either synthesized from cheap raw materials or are chosen from compounds having heteroatoms in their electron rich aromatic or long chain carbon system. The advantages of organic corrosion inhibitors include: presence of film prevents uniform corrosion attack;[10] organic inhibitors increase the activation energy on the metal surface (passivation); they have been shown to eliminate corrosion over a wide range of pH values. Organic inhibitors will be adsorbed according to the ionic charge of the inhibitor and the charge on the surface. The strength of the adsorption bond is the dominant factor for soluble organic inhibitors.

The effectiveness of these inhibitors depends on the chemical composition, their molecular structure, and their affinities for the metal surface.[11–13] Many investigators have been reported on the use of antibacterial drugs as corrosion inhibitors.[14–18] Inhibition efficiencies over 80 % were obtained for sparfloxacin from gravimetric, gasometric and thermometric methods for mild steel corrosion in HCl.[19] Inhibition properties of ampicilin for mild steel corrosion in H_2SO_4 and its synergistic combination with halides (I^-, Cl^-, Br^-) showed that inhibition efficiency increased with increasing concentration and halide presence, but decreased with rise in temperature.[20] Penicilin G was found to act as an inhibitor for the corrosion of mild steel. The adsorption of the inhibitor on the steel surface is physical, exothermic and spontaneous, and obeys Langmuir adsorption isotherm.[21] The corrosion inhibition of mild steel in HCl solution by streptomycin showed 88.5 % inhibition efficiency and has been studied by Tafel polarization, EIS and mass loss measurement.[22] These type of compounds are strongly basic and also very soluble in acidic media. Most of the drugs used play important roles in biological reactions because of their anticonvulsant, antibacterial, inhibitive to mycobacterium tuberculosis and other properties.[23,24]

The objective of this work is to study the corrosion inhibitive action of a sulfa drug, Sulfathiazole (TBSA) for the corrosion of carbon steel in 1.0 mol L^{-1} HCl. The choice of this drug as a corrosion inhibitor is based on its environmentally friendly property reportedly very important in biological reactions;[18] TBSA acts as antimicrobial agent by inhibiting bacterial growth; its molecule has S, O, N atoms as active centers.

*Corresponding author: Dr. Adriana Samide; Tel/Fax: +040251-597048;
E-mail address: samide_adriana@yahoo.com

Experimental

Materials

Materials used for the study were carbon steel sheet of composition (*w*/%): C = 0.12 %; Mn = 1 %; P = 0.045 %; S = 0.027 %, Fe remainder. HCl reagent used for the preparation of aggressive solutions was of AR grade. Appropriate concentrations of acid with and without adding inhibitor were prepared using distilled water. The antibacterial drug, Sulfathiazole (TBSA) was supplied by Fluka (purity > 98 %). Molecular structure of the used inhibitor is presented in Fig. 1.

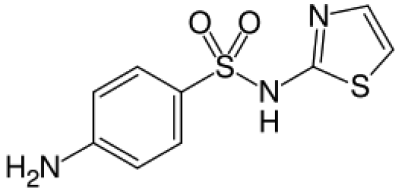

Fig. 1 – *Chemical molecular structure of 4-amino-N-(1, 3-thiazol-2-yl) benzene sulfonamide (TBSA)*

Mass loss method

Each sheet, with an area of 1 cm^2, successively polished with 200, 600, 800 grade of emery paper was degreased by washing in acetone, ultrasonically cleaned with bi-distilled water and preserved in a vacuum dessicator. After accurately weighting, the specimens were immersed in a beaker containing 100 mL HCl with and without addition of different concentrations of TBSA. The concentration of HCl used was 1.0 mol L^{-1} while the concentrations of the inhibitor were: $5 \cdot 10^{-4}$ mol L^{-1}; $7 \cdot 10^{-4}$ mol L^{-1}; $9 \cdot 10^{-4}$ mol L^{-1}; $11 \cdot 10^{-4}$ mol L^{-1} (0.5 mmol L^{-1}; 0.7 mmol L^{-1}; 0.9 mmol L^{-1}; 1.1 mmol L^{-1}). Mass loss was measured at room temperature. After 6 hours, the specimens were taken out, washed, dried, and weighed accurately. The average mass loss of the carbon steel sheets could be obtained.

Electrochemical measurements

Electrochemical measurements were performed using a Voltalab 40 model PGZ301 potentiostat/galvanostat conducted by a personal computer with VoltaMaster 4 software. A typical three-electrode cell with a working electrode made of carbon steel with an active surface of 1 cm^2 was used. The auxiliary electrode was a platinum plate (1 cm^2) and the reference electrode was represented by a saturated Ag/AgCl electrode. Potentiodynamic polarization curves were obtained with the scan rate of 1 mV s^{-1}, in a potential range from –700 mV to –100 mV. The immersion time of the plates in the respective media was 4 minutes in open circuit, at room temperature.

Electrochemical impedance spectroscopy (EIS) measurements were carried out after 6 h, at the open circuit potential (E_{ocp}), in a frequency range from 10^5 Hz to 10^{-1} Hz by a parturition signal of 10 mV amplitude peak to peak, at room temperature.

Potentiodynamic polarization and EIS data were analyzed by means of *Excel* and *Zview*, respectively.

Surface characterization

The morphologies of the surfaces were inspected by SEM on Vega Tescan scanning electron microscope, resolution 60 Angstroms, magnification range: 10 X – 180 000 X, SE detector.

XPS spectra were recorded in a VG ESCA 3 Mk II- EUROSCAN spectrometer with a Mg K_ X-ray source (1486.7 eV photons energy) operated at 300 W (accelerating voltage 12.5 kV, emission current 24 mA). The pressure in the analysis chamber did not exceed the value of $2.66 \cdot 10^{-6} – 4 \cdot 10^{-6}$ Pa during the entire period of spectra acquisition. In order to perform the surface charge compensation, a FG40 flood gun device (Specs Gmbh – Germany), was used, with a 0.1 mA electronic current at 2 eV energy. The samples were measured in an "as received" condition with no other surface cleaning treatment (chemical etching or Ar^+ ion beam bombardment). Survey spectra were recorded with a window of 1250 eV and 100 eV pass energy. All spectra were deconvoluted with SDP 2.3 XPS-International software, using Gaussian profile lines for peak fitting.

Results and discussion

Mass loss measurements

The mass loss of carbon steel samples in 1.0 mol L^{-1} HCl in the absence and in the presence of various concentrations of TBSA was determined. The results of mass loss measurements are shown as general corrosion rates W (g m^{-2} h^{-1}) in Fig. 2. The increase in TBSA concentration leads to a decrease in the corrosion rate, indicating that the presence of TBSA retards the general corrosion of samples in 1.0 mol L^{-1} HCl. This suggests that the inhibition of the carbon steel corrosion in the presence of TBSA occurs by adsorption at site on the metal surface. The molecular structure, type and concentration of inhibitor, mode of adsorption, chemical nature of "anchoring" and the composition of steel determine the efficiency of inhibitors. The molecules of TBSA may be adsorbed on the metal sur-

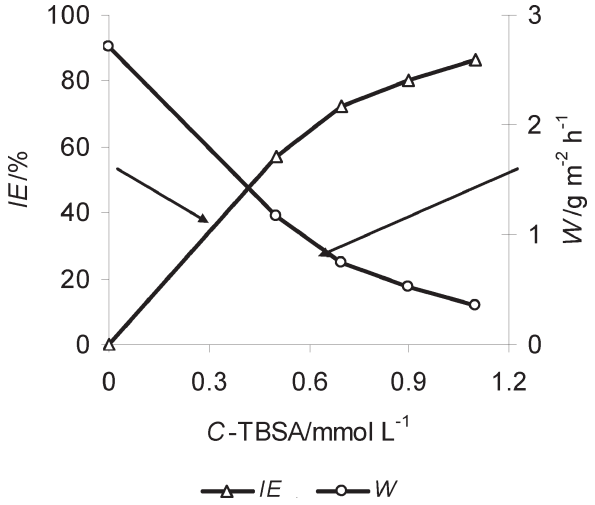

F i g . 2 – *Corrosion rate and inhibition efficiency of carbon steel corroded in 1.0 mol L^{-1} HCl solution in the absence and presence of TBSA, at room temperature*

face through interactions between the pair of non-participating electrons from the nitrogen and the sulfur (from thiazolic ring) atoms of the TBSA molecule and the carbon steel substrate. The effect of surface blockage becomes dominant, which leads to a decrease in the active centers. The inhibition efficiency increased with in the increase in TBSA concentration. The percentage inhibition efficiency (*IE*/%) of TBSA was calculated applying the following equation:

$$IE = \frac{W_{free} - W_{inh}}{W_{free}} \cdot 100 \qquad (1)$$

where W_{free} and W_{inh} are, respectively, the corrosion rates in the absence and presence of a given inhibitor. The inhibition efficiencies calculated from the mass loss data are given in Fig. 2.

Adsorption isotherm

One of the most convenient ways of expressing adsorption quantitatively is by deriving the adsorption isotherm that characterizes the metal/inhibitor/environment system. Various adsorption isotherms were applied to fit θ values, but the best fit was found to obey Temkin adsorption isotherm, which may be expressed by:

$$\theta = \frac{2.303}{f} \cdot \log K + \frac{2.303}{f} \cdot \log c \qquad (2)$$

where c is the concentration (mol L^{-1}) of the inhibitor in the bulk electrolyte, θ is the degree of surface coverage ($\theta = IE/100$), K is the adsorption equilibrium constant and f is the number of the surface active sites occupied by one inhibitor molecule.

Plotting θ against *log c* for the TBSA is given in Fig. 3, where a straight-line relationship was obtained suggesting the validity of this model for the studied case. The result obtained indicates that the R^2 value for the plots is very close to unity, which indicates a strong adherence of the assumptions of Temkin to experimental data. The slope of this line equals 2.303/*f* and the intercept is [(2.303/*f*) · log K], from which the value of K was calculated. It can be observed that K has a value of 260250 L mol^{-1} and f = 3.23. It is noted that the value of "*f*" is more than unity. This means that the given inhibitor molecules will form a monolayer on the steel surface.

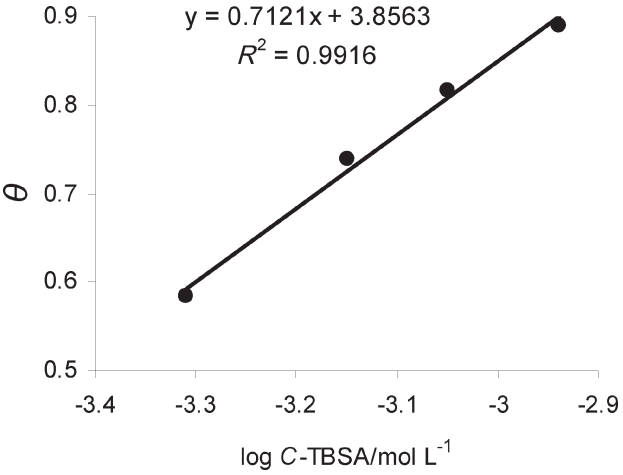

F i g . 3 – *Temkin adsorption plots of carbon steel corroded in 1.0 mol L^{-1} HCl solution containing various concentrations of TBSA, at room temperature*

The equilibrium constant of adsorption K obtained from the intercepts of Temkin adsorption isotherm is related to the free energy of adsorption ΔG_{ads}^0 as follows:

$$K = \frac{1}{55.5} \exp\left(-\frac{\Delta G_{ads}^0}{R \cdot T}\right) \qquad (3)$$

where R is the universal gas constant, T is temperature (K) and 55.5 is the molar concentration of water in the solution.

The negative value (–40.824 kJ mol^{-1}) obtained for ΔG_{ads}^0 suggests that the inhibitor's molecules are adsorbed on the carbon steel surface. The values also indicate a spontaneous adsorption of the inhibitor molecules and usually characterize their strong interaction with the metal surface. The value of ΔG_{ads}^0 of (–40 kJ mol^{-1}) is usually accepted as a threshold value between chemical and physical adsorption. The value of ΔG_{ads}^0 obtained in our study (–40.824 kJ mol^{-1}) indicates a chemical adsorption mechanism.

Electrochemical measurements

Potentiodynamic curves

Potentiodynamic anodic and cathodic polarization scans were carried out at room temperature in 1.0 mol L^{-1} HCl blank solution and 1.0 mol L^{-1} HCl containing different concentrations of TBSA (Fig. 4).

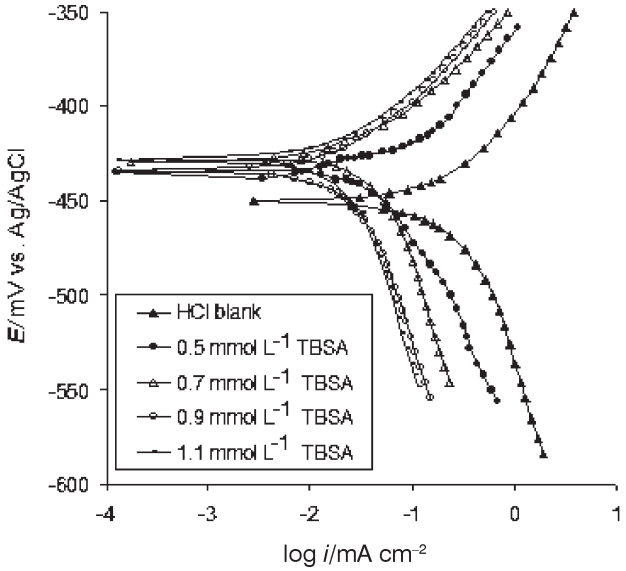

Fig. 4 – *Potentiodynamic curves of carbon steel corroded in 1.0 mol L^{-1} HCl solution with and without various concentrations of TBSA, at room temperature*

From Fig. 4 it can be seen that, in the presence of the inhibitor, the curves are shifted to lower current regions, showing the inhibition tendency of TBSA. Also, the presence of TBSA in the corrosive medium increases the anodic and cathodic over-potentials. This shows that TBSA addition reduces anodic dissolution and delays the hydrogen evolution reaction. The presence of this inhibitor in 1.0 mol L^{-1} HCl solution disturbs significantly the cathodic reaction and reduces the anodic reaction in a considerable manner. TBSA acts as a corrosion inhibitor in 1.0 mol L^{-1} HCl solution by suppressing simultaneously the cathodic and anodic processes *via* adsorption on the carbon steel surface.

The corrosion current density (i_{corr}) was calculated at intercept of the anodic and cathodic Tafel lines to corrosion potential, using VoltaMaster 4 software (see Table 1).

The results showed that the corrosion current density decreased with the increase in TBSA concentration, which indicates that this compound acts as inhibitor by adsorption onto steel surface, and the inhibition degree depends on the TBSA concentration. The percentage inhibition efficiency (*IE*) of

Table 1 – *Electrochemical parameters and inhibition efficiency (IE) obtained for carbon steel in 1.0 mol L^{-1} HCl solution with and without different concentrations of TBSA at room temperature*

Medium	E_{corr} (mV vs. Ag/AgCl)	i_{corr} (mA cm^{-2})	R_p (Ω cm^2)	*IE* (%)
HCl blank solution	–450	0.429	69.2	0
HCl/0.5 mmol L^{-1} TBSA	–435	0.179	165.9	58.3
HCl/0.7 mmol L^{-1} TBSA	–434	0.102	293.2	76.4
HCl/0.9 mmol L^{-1} TBSA	–429	0.079	376.1	81.6
HCl/1.1 mmol L^{-1} TBSA	–428	0.052	571.9	87.9

TBSA was also determined from the polarization measurements according to the following equation:

$$IE = \frac{i^0_{corr} - i_{corr}}{i^0_{corr}} \cdot 100 \qquad (4)$$

where i^0_{corr} and i_{corr} are the corrosion current densities of carbon steel in 1.0 mol L^{-1} HCl solution without and with TBSA, respectively.

The polarization curves obtained in the potential ranges near to corrosion potentials were recorded with a scan rate of 1 mV s^{-1}. The linearization was accomplished in the domain of over-voltages values of ± 10 mV (Fig. 5).

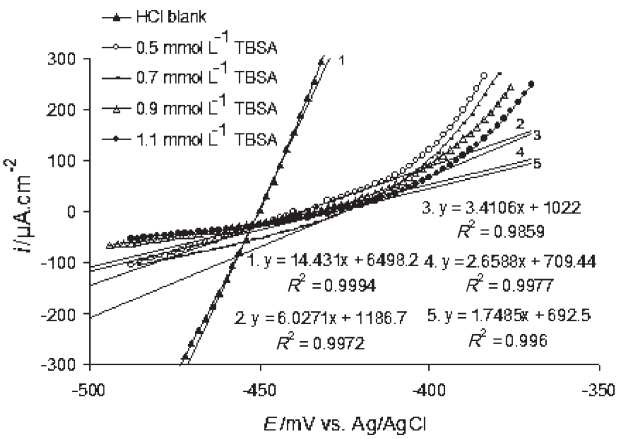

Fig. 5 – *Polarization resistance (R_p) of carbon steel corroded in 1.0 mol L^{-1} HCl solution in absence and in presence of TBSA in different concentrations: 0.5 mmol L^{-1}; 0.7 mmol L^{-1}; 0.9 mmol L^{-1}; 1.1 mmol L^{-1}*

The slopes $(di/dE)_{E \to Ecorr}$ of the lines from Fig. 5, represent the polarization conductance. Polarization resistance ($R_p/k\Omega$ cm^2) was calculated using relation 5.

$$\left(\frac{di}{dE}\right)_{E \to E_{corr}} = \frac{1}{R_p} \qquad (5)$$

The study of the response of carbon steel given by polarizing in HCl solution without and with TBSA, showed a shift in polarization resistance (R_p) to higher values, with the increase in TBSA concentration (Fig. 5 and Table 1). This suggests that the corrosion inhibition of the carbon steel corrosion in the presence of TBSA occurs by adsorption on the metal surface. The numerical values of the electrochemical parameters on the behaviour of carbon steel in 1.0 mol L^{-1} HCl solution and 1.0 mol L^{-1} HCl solution containing different concentrations of TBSA were calculated using VoltaMaster 4 software with an error of ± 1.5 %, and are presented in Table 1.

Table 1 reveals that the values of inhibition efficiency increase with TBSA concentration, reaching a maximum of 87.9 %, at 1.1 mmol L^{-1} TBSA concentration, almost equal to the value obtained from mass loss measurements (86.7 %).

Electrochemical impedance spectroscopy

Fig. 6 shows the impedance measurements of carbon steel electrode in 1.0 mol L^{-1} HCl solution and in 1.0 mol L^{-1} HCl containing TBSA in different concentrations: 0.5 mmol L^{-1}; 0.7 mmol L^{-1}; 0.9 mmol L^{-1}; 1.1 mmol L^{-1} vs. Ag/AgCl reference electrode, in the frequency range from 10^5 to 10^{-1} Hz with a value of 10 mV for the amplitude, at open circuit potential (E_{ocp}). The impedance spectrum is represented as a Nyquist diagram with a capacitive loop more or less leveled, which presents a phase shift comparative with the real axe. This is due to the density variations of the electrode surface coating. Furthermore, the Nyquist plots shape for carbon steel in the solutions with and without inhibitor are not perfect semicircles from EIS theory in the frequency range. This difference is characteristic for solid electrodes and usually refers to frequency dispersion, which is attributed to roughness and other inhomogeneities of solid electrode surface.

The protective properties of the layer increase with increasing diameter of the semicircle.

It is clear that TBSA presence produced a higher polarization resistance value, which is interpreted in terms with the formation of an effective protective layer that diminishes the corrosion processes.

For the description of EIS measurements an equivalent circuit is suggested in Fig. 7, where (R_s) is the solution resistance of the bulk electrolyte and (C_{dl}) represents the double layer capacitance of the electrolyte at the metal surface. Because of the inhomogeneities in the coating, this capacitance is implemented as a Constant Phase Element (CPE). (R_p) is the polarization resistance of the metal. The CPE is defined by:

$$Z_{CPE} = 1/[T\ (j\omega)^P] \quad (6)$$

where: ω is the angular frequency and $j^2 = -1$. When the exponent P = 1, a CPE is identical to a capacitor and T = C. For P = 0, a CPE is equivalent to a resistor and T = 1/R. At intermediate values of P, the CPE is a phenomenological term with no simple physical justification.

The impedance parameters derived from EIS measurements and respective fitting results are given in Table 2 and Fig. 7 respectively.

The fitting results show that R_s and C_{dl} –T decrease and R_p increases. This suggests that the amount of adsorbed TBSA molecules increases. This decrease in C_{dl} –T could be attributed to the decrease in local dielectric constant and/or increase in the thickness of the electrical double layer, signi-

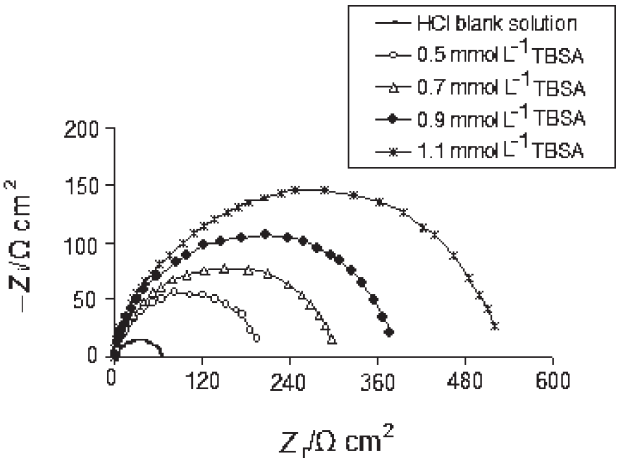

Fig. 6 – *Nyquist plots for carbon steel in 1.0 mol L^{-1} HCl solution with and without different concentrations of TBSA, after 6 hours, at room temperature*

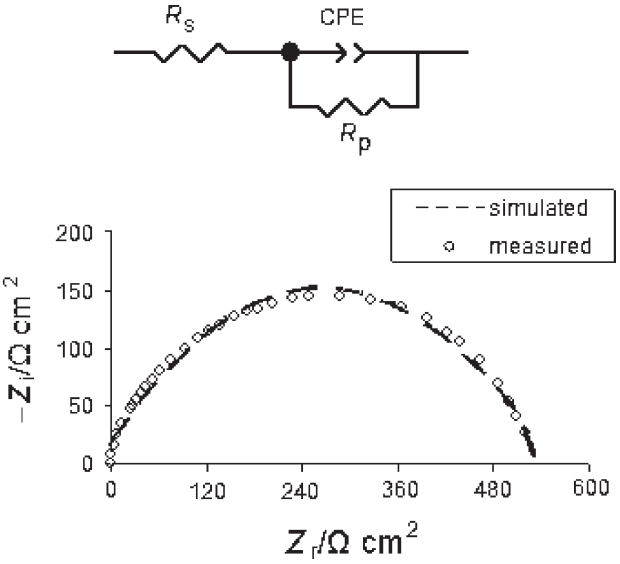

Fig. 7 – *Equivalent circuit model for the studied inhibitor and Nyquist plots for carbon steel in 1.0 mol L^{-1} HCl solution containing 1.1 mmol L^{-1} TBSA (○: measurement ; – –: fitting result)*

Table 2 – *Impedance parameters for carbon steel in 1.0 mol L^{-1} HCl solution in the absence and in the presence of different concentrations of TBSA at room temperature, after 6 h of immersion time*

C-TBSA (mmol L^{-1})	E_{corr} (mV vs. Ag/AgCl)	R_s (Ω cm^2)	C_{dl}-T (μF cm^{-2})	C_{dl}-P (μF cm^{-2})	R_p (Ω cm^2)	*IE* (%)
0	–453	2.897	548.0	0.73	84.2	0
0.5	–441	2.627	443.2	0.78	238.6	64.7
0.7	–436	2.359	382.2	0.79	371.5	77.3
0.9	–430	1.998	311.6	0.81	422.7	80.1
1.1	–426	1.785	275.1	0.85	582.9	85.5

fying that the TBSA acts by adsorption at the interface of metal/solution. Values approaching 1 of the exponent P of C_{dl} –P, indicate a pseudo-capacity for the double layer, in the presence of TBSA, which certainly is less porous than once P of C_{dl} –P is more deviated from 1, in the absence of inhibitor (Table 2). R_p was used to calculate the inhibition efficiency from eq. 7.

$$IE = \frac{R_p - R_p^0}{R_p} \cdot 100 \qquad (7)$$

where R_p and R_p^0 represents the polarization resistances in the presence and absence of inhibitor, respectively.

The presence of TBSA leads to an approx. 85.5 % inhibition efficiency, a closer value to that obtained from mass loss and potentiodynamic curves (see Table 2).

Surfaces characterization

After mass loss measurements, the corroded samples in 1.0 mol L^{-1} HCl solution without and with TBSA were also examined using SEM and XPS surface analysis. The best inhibition occurred when the TBSA concentration was 1.1 mmol L^{-1}.

SEM observation

The SEM images of carbon steel surface before corrosion (Fig. 8a) and after occurrence of the corrosive processes in 1.0 mol L^{-1} solution (Fig. 8b) and in 1.0 mol L^{-1} HCl solution containing 1.1 mmol L^{-1} TBSA (Fig. 8c) are presented.

When carbon steel was corroded in 1.0 mol L^{-1} HCl solution without inhibitor, random spread corrosion spots could be noticed (Fig. 8b). When TBSA was used, the texture was modified and the corrosion spots had low intensity. It can be observed that the surface morphology shown in the presence of TBSA (Fig. 8c) is significantly different and more regular than that obtained in 1.0 mol L^{-1} HCl without TBSA (Fig. 8b).

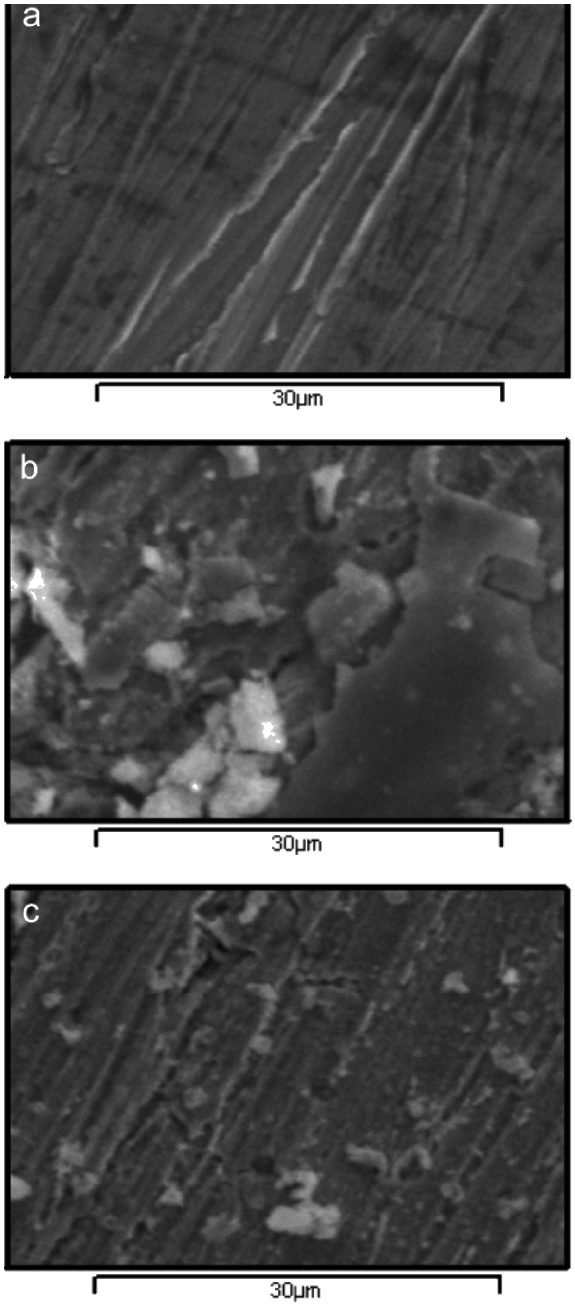

Fig. 8 – *SEM images of carbon steel: a- before corrosion; after corrosion in: b – in 1.0 mol L^{-1} HCl solution without TBSA; c – in 1.0 mol L^{-1} HCl solution containing 1.1 mmol L^{-1} TBSA*

Table 3 – *XPS parameters measured on the Fe 2p, O 1s, N 1s and S 2p levels for carbon steel corroded in 1.0 mol L^{-1} HCl blank solution and 1.0 mol L^{-1} HCl solution containing 1.1 mmol L^{-1} TBSA*

	C – steel/HCl blank			C – steel/HCl/TBSA		
	BE/eV	FWHM/eV	Counts	BE/eV	FWHM/eV	Counts
Fe^{3+}	710.7	3.79	76959.5	710.8	3.63	49929
O^{2-}	718.8	1.05	322.4	718.9	1.14	603.5
	530.0	2.47	72721.7	530.0	2.24	69459.2
OH^-	531.6	2.38	62354.2	531.5	1.88	52112
O_{ads}	533.8	1.46	2082.8	532.9	2.24	25629
N 1s	–	–	–	399.9	3.04	3400.4
S 2p	–	–	–	164.7	3.94	376.02
	–	–	–	169.3	3.22	359.06

XPS surface composition

Fe $2p^{3/2}$ energy levels were monitored by XPS on the surface of carbon steel samples corroded in 1.0 mol L^{-1} HCl blank solution and 1.0 mol L^{-1} HCl solution containing 1.1 mmol L^{-1} TBSA. Note that the XPS parameters measured on the Fe 2p, O 1s, N 1s and S 2p levels are given in Table 3.

$Fe^{3+}(2p^{3/2})$ appeared at 710.7 eV for the sample that was corroded in 1.0 mol L^{-1} HCl blank solution, and at 710.8 eV, in case where the carbon steel was corroded in the presence of TBSA. The positions and energy are very close to that observed either for FeO(OH) or Fe_2O_3 structures.[25] The satellites that appeared at 718.8 eV and 718.9 eV respectively, are also characteristic of Fe^{3+}. The spectra are displayed in Figs. 9a and 10a.

Estimation of the relative XPS peak intensities of oxidized iron in carbon steel shows the decrease of the iron oxide/oxyhydroxide fraction in corroded sample in 1.0 mol L^{-1} HCl solution containing TBSA. In order to differentiate between FeO(OH) and Fe_2O_3 we also monitored the O(1s) region.

The whole set of comparable binding energies obtained for the O 1s peak (Figs. 9b and 10b) deserves some comment. On the high binding energy side, precise assignments are difficult in relation to the existence of ionizations associated with adsorbed species.[26] The analyses have shown: from 530.5 to 531.1 eV, ionization characteristics of oxygen species integrated into the material as O^{2-} and OH^-, respectively; from 531.1 to 532 eV, ionization of oxygen species that could allow compensation for some deficiencies in the subsurface of metal oxides. Formally, these oxide ions could be described as O^- species – indeed, owing to a higher covalence of the M-O bonds, these low-coordinated oxygen ions could be characterized by a lower electron density than classical O^{2-} ions.[26]

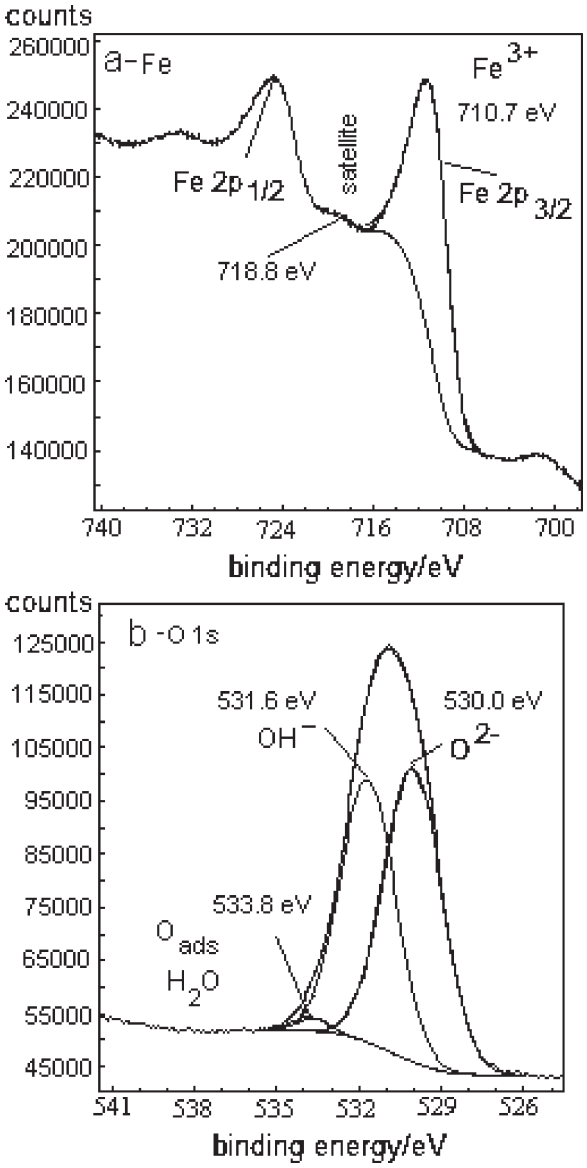

Fig. 9 – *XPS spectra of carbon steel corroded in 1.0 mol L^{-1} HCl solution without TBSA: a – iron spectrum; b – O 1s spectrum*

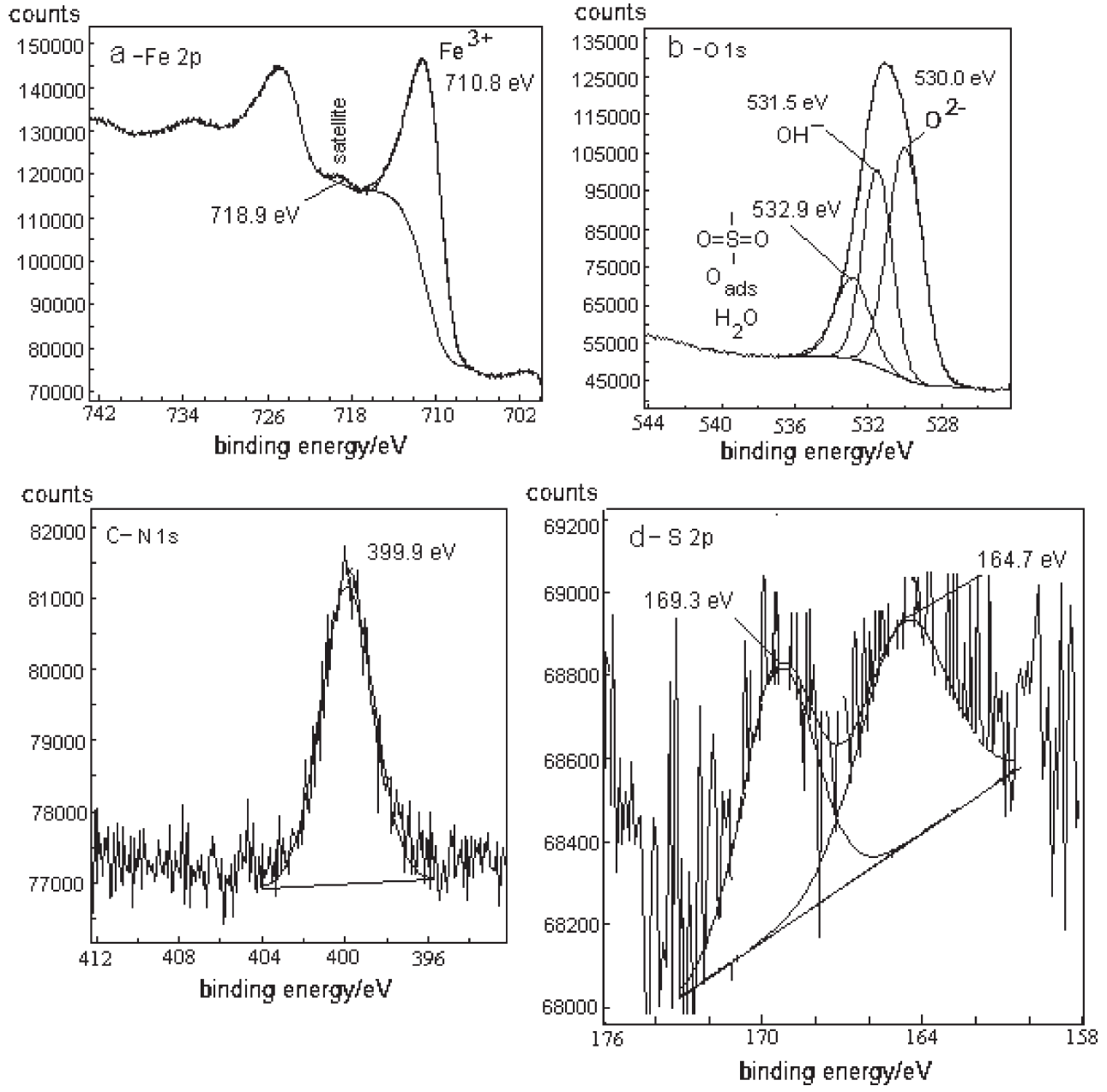

Fig. 10 – *XPS spectra of carbon steel corroded in 1.0 mol L^{-1} HCl solution containing 1.1 mmol L^{-1} TBSA: a – iron spectrum; b – O 1s spectrum; c – N 1s spectrum; d – S 2p spectrum*

For the samples corroded in HCl blank solution and in HCl solution containing TBSA the oxygen peak could be deconvoluted to three components with peak positions at 530.0, 531.6 eV, 533.8 eV and 530.0, 531.5 eV, 532.9, respectively, related to metal oxides and hydroxides, O=S=O/C=O bonds[27,28] or other adsorbed species such as oxygen from the water.[26] For FeO(OH) two well resolved peaks were observed at 530.0 (O^{2-}) and 531.6 / 531.5 eV (OH^-). The O 1s for Fe_2O_3 was found at 530.0 eV. Taking these data into account, we may conclude that the surface layer consists of FeO(OH) rather than pure oxide. Iron oxyhydroxide may occur in anhydrous (FeO(OH)) or hydrated ($FeO(OH)\cdot nH_2O$) forms. The monohydrate ($FeO(OH)\cdot H_2O$) might otherwise be described as iron(III) hydroxide ($Fe(OH)_3$), and is also known as hydrated iron oxide or yellow iron oxide. From Table 4 it can be observed that the oxide/oxyhydroxide amount decreased in the presence of inhibitor. Moreover, the adsorbed species amount increased, related to sulfone ($-SO_2-$) group presence.

Further relevant information about the chemical composition of surface corroded in 1.0 mol L^{-1} HCl solution containing TBSA is obtained from the XPS spectral analysis of N 1s and S 2p photo-peaks (Figs. 10c and 10d).

Table 4 – *Composition of layer deposited on carbon steel surface measured by XPS for carbon steel corroded in 1.0 mol L^{-1} HCl blank solution and 1.0 mol L^{-1} HCl solution containing 1.1 mmol L^{-1} TBSA*

Sample	Fe2p$^{3/2}$	O 1s (O^{2-})	O 1s (OH^-)	O 1s (ads)	N 1s	S 2p
C-steel/HCl blank	Fe^{3+}	530.0 eV	531.6 V	533.8 eV	–	–
		53 %	**45.4 %**	**1.6 %**	–	–
C-steel/HCl/TBSA	Fe^{3+}	530.0 eV	531.5 eV	532.9 eV	399.9 eV	164.7 eV 169.4 eV
		47.2 %	**35.4 %**	**17.4 %**	–	–

The spectral simulation of the N 1s photo-peak (Fig. 10c) for carbon steel corroded in the presence of TBSA shows organic nitrogen species at 399.9 eV such as amine, amide, imine, etc.[29] Indeed, this binding energy corresponds to amine group from TBSA molecule and/or C-N bonds and/or this can be attributed at the unprotonated N atoms (=N- structure) in the thiazolic ring.

The S 2p level spectra (Fig. 10d) consist of two sets of peaks: at low binding energies (164.7 eV) and at higher binding energy (169.4 eV). Photo-peak at high binding energies (169.4 eV) corresponds to highly oxidized (+VI) sulfur such as sulfone,[29] from the TBSA molecule. Photo-peak at low binding energies (164.7 eV) is attributed to organic sulfur entities that are close to neutral sulfur. Corresponding organic species may be thiophenes and disulfides.[29] Thus, we attributed this peak to organic sulfur from thiazolic ring, which is present in the TBSA molecule.

Conclusions

TBSA inhibits corrosion of carbon steel in 1.0 mol L^{-1} HCl solution; it has an efficiency of 86.7 ± 1 % obtained from mass loss data and electrochemical measurements. SEM indicated that the surface morphology shown in the presence of TBSA is significantly different and more regular than that obtained in 1.0 mol L^{-1} HCl solution without TBSA. XPS analysis confirms the adsorption of inhibitor on carbon steel surface and shows that in the presence of TBSA the corrosion process is decelerated; at this stage, the main product of corrosion is a non-stoichiometric Fe^{3+} oxide/oxyhydroxide, consisting of a mixture of FeO(OH) and Fe_2O_3, where FeO(OH) is the main phase. This is interpreted in terms of the formation of a protective layer consisting of organic film and an amount of iron compounds.

ACKNOWLEDGEMENTS

This work was supported by CNCSIS –UEFISCSU, project number PNII – IDEI 422/2008. The authors thank the IDEI/Grant-Program, 422/2008 competition.

List of symbols

TBSA – 4-amino-N-(1, 3-thiazol-2-yl) benzene sulfonamide
EIS – electrochemical impedance spectroscopy
XPS – X-ray photoelectron spectroscopy
SEM – scanning electron microscopy
W – corrosion rate, g m^{-2} h^{-1}
W_{free} – corrosion rate in the absence of the inhibitor, g m^{-2} h^{-1}
W_{inh} – corrosion rate in the presence of the inhibitor, g m^{-2} h^{-1}
IE – inhibition efficiency, %
E_{ocp} – open circuit potential, mV
E_{corr} – corrosion potential, mV
θ – surface coverage degree
K – adsorption equilibrium constant
c – molar concentration, mol L^{-1}
f – number of the surface active sites occupied by one inhibitor molecule
ΔG^0_{ads} – free energy of adsorption, kJ mol^{-1}
R – universal gas constant, 8.314 J mol^{-1} K^{-1}
T – temperature, K
i_{corr} – corrosion current density, mA cm^{-2}
i^0_{corr} – corrosion current density in the presence of the inhibitor, mA cm^{-2}
R_p – polarization resistance in the presence of the inhibitor, Ω cm^2
$R_p{}^0$ – polarization resistance in the absence of the inhibitor, Ω cm^2
R_s – solution resistance, Ω cm^2
CPE – Constant Phase Element
C_{dl} – double layer capacitance, μF cm^{-2}
BE – binding energy, eV

References

1. *Larabi, L., Harek, Y., Traisnel, M., Mansria, A.,* J. Appl. Electrochem. **34** (2004) 833.
2. *Samide, A., Bibicu, I., Rogalski, M. S., Preda, M.,* Corros. Sci. **47** (2005) 1119.
3. *Abdallah, M.,* Corros. Sci. **46** (2004) 1981.
4. *Ashassi-Sorkhabi, H., Ghasemi, Z., Seifzadeh, D.,* Appl. Surf. Sci. **249** (2005) 408.

5. *Samide, A., Bibicu, I.,* Surf. Interf. Analysis **40** (2008) 944.
6. *El-Rehim, S. S. A., Refaey, S. A. M., Taha, F., Saleh, M. B.,* J. Appl. Electrochem. **31** (2001) 429.
7. *Samide, A., Bibicu, I., Agiu, M., Preda, M.,* Mater. Lett. **62** (2008) 320.
8. *Samide, A., Bibicu, I., Rogalski, M. S., Preda, M.,* J. Radioanal. Nucl. Chem. **261** (2004) 593.
9. *Milošev, I., Kosec, T.,* Chem. Biochem. Eng. Q. **23** (2009) 53.
10. *Otmačić Ćurković, H., Marušić, K., Stupnišek-Lisac, E., Telegdi, J.,* Chem. Biochem. Eng. Q. **23** (2009) 61.
11. *Hassan, N., Holze, R.,* J. Chem. Sci. **121** (2009) 693.
12. *Samide, A., Turcanu, E., Bibicu, I.*, Chem. Eng. Comm. **196** (2009) 1008.
13. *Fouda, A. S., Mostafa, H. A., El-Abbasy, H. M.,* J. Appl. Electrochem. **40** (2010) 163.
14. *Obot, I. B., Obi Egbedi, N. O.,* Corros. Sci. **52** (2010) 282.
15. *Shukla, S. K., Singh, A. K., Ahamad, I., Quraishi, M. A.,* Mater. Lett. **63** (2009) 819.
16. *El-Naggar, M. M.,* Corros. Sci. **49** (2007) 2226.
17. *Samide, A., Tutunaru, B., Negrila, C., Trandafir, I., Maxut, A*., Digest J. Nanomater. Biostruct. **6** (2011) 663.
18. *Ebenso, E., Arslan, T., Kandemirli, F., Love, I., Ödretir, C., Saracoğlu, M., Umoren, S. A.,* Int. J. Quantum Chem. **110** (2010) 2614.
19. *Eddy, N. O., Odoemelam, S. A., Mbaba, A. J.,* African J. Pure and Appl. Chem. **2** (2008) 132.
20. *Eddy, N. O., Ebenso, E. E., Ibok, U. J.,* J. Appl. Electrochem. **40** (2010) 445.
21. *Eddy, N. O., Odoemelam, S. A., Ekwumemgbo, P.,* Sci. Res. Essay **4** (2009) 33.
22. *Hosseini, M. G., Ehteshamzadeh, A., Shahrabi, T.,* Electrochim. Acta **52** (2007) 3680.
23. *Sing, W. T., Lee, C. L., Yeo, S. L., Lim, S. P., Sim, M. M.,* Bioorg. Med. Chem. Lett. **11** (2001) 91.
24. *El-Dissouky, A., El-Bindary, A. A., El-Soubati, A. Z., Hilali, A. S.,* Spectrochim. Acta. Part A. **57** (2001) 1163.
25. *Grosvenor, A. P., Kobe, B. A., Biesinger, M. C., McIntyre, N. S.,* Surf. Interf. Analysis **36** (2004) 1564.
26. *Dupin, J. C., Gonbeau, D., Vinatier, P., Levasseur, A.,* Phys. Chem. Chem. Phys. **2** (2000) 1319.
27. *Yi, Z. A., Xu, Y. Y., Zhu, L. P., Dong, H. B, Zhu, B. K.,* Chinese. J. Polymer Sci. **27** (2009) 695.
28. *Vinnichenko, M., Chevolleau, T., Pham, M. T., Poperenko, L., Maitz, M. F.,* Appl. Surf. Sci. **201** (2002) 41.
29. *Billon, G., Ouddane, B., Gengembre, L., Boughriet, A.,* Phys. Chem. Chem. Phys. **4** (2002) 751.